ACS APPLIED MATERIALS & INTERFACES

Research Article

www.acsami.org

RGD Peptide-Modified Dendrimer-Entrapped Gold Nanoparticles Enable Highly Efficient and Specific Gene Delivery to Stem Cells

Lingdan Kong,[†] Carla S. Alves,[‡] Wenxiu Hou,[†] Jieru Qiu,[†] Helmuth Möhwald,[§] Helena Tomás,*[,‡] and Xiangyang Shi*[,†,‡]

[†]College of Chemistry, Chemical Engineering and Biotechnology, Donghua University, Shanghai 201620, People's Republic of China

[‡]CQM-Centro de Química da Madeira, Universidade da Madeira, Campus da Penteada, 9000-390 Funchal, Portugal

[§]Max-Planck Institute of Colloids and Interfaces, Golm-Potsdam 14476, Germany

Supporting Information

ABSTRACT: We report the use of arginine-glycine-aspartic (Arg-Gly-Asp, RGD) peptide-modified dendrimer-entrapped gold nanoparticles (Au DENPs) for highly efficient and specific gene delivery to stem cells. In this study, generation 5 poly(amidoamine) dendrimers modified with RGD via a poly(ethylene glycol) (PEG) spacer and with PEG monomethyl ether were used as templates to entrap gold nanoparticles (AuNPs). The native and the RGD-modified PEGylated dendrimers and the respective well characterized Au DENPs were used as vectors to transfect human mesenchymal stem cells (hMSCs) with plasmid DNA (pDNA) carrying both the enhanced green fluorescent protein and the luciferase (pEGFPLuc) reporter genes, as well as pDNA encoding the human bone morphogenetic protein-2 (hBMP-2) gene. We show that all vectors are capable of transfecting the hMSCs with both pDNAs. Gene transfection using pEGFPLuc was demonstrated by quantitative Luc activity assay and qualitative evaluation by fluorescence microscopy. For the transfection with hBMP-2, the gene delivery efficiency was evaluated by monitoring the hBMP-2 concentration and the level of osteogenic differentiation of the hMSCs via alkaline phosphatase activity, osteocalcin secretion, calcium deposition, and von Kossa staining assays. Our results reveal that the stem cell gene delivery efficiency is largely dependent on the composition and the surface functionality of the dendrimer-based vectors. The coexistence of RGD and AuNPs rendered the designed dendrimeric vector with specific stem cell binding ability likely via binding of integrin receptor on the cell surface and improved three-dimensional conformation of dendrimers, which is beneficial for highly efficient and specific stem cell gene delivery applications.

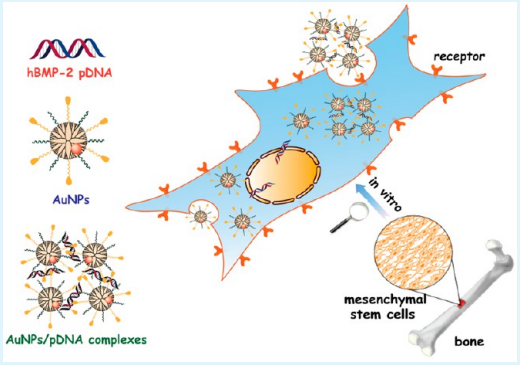

KEYWORDS: *dendrimers, gold nanoparticles, gene delivery, stem cells, osteogenic differentiation*

INTRODUCTION

Human mesenchymal stem cells (hMSCs) are multipotent cells that display immunosuppressive properties and have an inherent ability to differentiate into various types of cells, including osteoblasts, myocytes, chondrocytes, and adipocytes.[1−5] Moreover, as a result of their strong expansion capabilities, hMSCs hold great promise for the construction and regeneration of damaged tissues.[6,7] Based on these properties, hMSCs have been considered as an excellent vehicle for gene therapy. For successful gene therapy applications, it is crucial to develop a suitable nonviral vector system with low cytotoxicity, high gene transfection efficiency, and specificity to diseased cells.

The feasibility of using dendrimers for human mesenchymal stem cell (hMSC) gene delivery has been recently demonstrated.[8−10] Dendrimers are a class of highly branched, monodispersed, synthetic macromolecules with spherical geometry, accurate molecular structure, and abundant surface functional groups.[11,12] The unique properties of dendrimers afford their successful uses in cancer diagnosis,[13−19] drug delivery,[20−26] and gene therapy.[27−32] Due to the polycationic character and the challenges posed by the practical gene delivery applications (e.g., low gene transfection efficiency and nonspecificity), it is essential to chemically modify the dendrimer surfaces or alter the internal structural characteristics for noncytotoxic, high-efficiency, and specific gene delivery applications.

For gene delivery with minimal cytotoxicity, it is prerequisite to modify the dendrimer surface to decrease the number of amine groups and thus diminish dendrimer cationic character. Partial modification with poly(ethylene glycol) (PEG) has been considered as a promising strategy to improve the biocompatibility of dendrimers.[15,16,33−37] It has been demonstrated that PEG-conjugated poly(amidoamine) (PAMAM) dendrimers

Received: December 11, 2014
Accepted: February 6, 2015
Published: February 6, 2015

DOI: 10.1021/am508760w
ACS Appl. Mater. Interfaces 2015, 7, 4833−4843

possess reduced cytotoxicity and improved gene transfection efficiency.[38] This is because PEG possesses the ability to reduce nonspecific interactions with serum proteins, as well as avoids recognition by the immune system. This has been also successfully demonstrated by PEG conjugation with oligonucleotides,[39] peptides,[40] and nanoparticles (NPs).[41,42]

For specific gene delivery applications, it is promising to modify the dendrimer surface with targeting ligands that can recognize the target cells via specific ligand−receptor interaction.[32] The cell surface integrin receptors which are overexpressed in many types of cells including hMSCs, glioblastoma cells, ovarian cancer cells, and breast cancer cells[43−45] have been shown to have a high affinity to bind arginine-glycine-aspartic (Arg-Gly-Asp, RGD) peptide.[38] Therefore, RGD peptide has been identified as a promising targeting ligand for different biomedical applications.[17] Dendrimers modified with RGD peptide have been demonstrated to have binding specificity to integrin-overexpressing cancer cells for drug delivery[46,47] and specific gene delivery[9] applications.

Besides the strategy of dendrimer surface modification, to increase the gene delivery efficiency of dendrimer-based vectors, the dendrimers should maintain well their three-dimensional (3D) conformation, thus having improved DNA compaction capability. Our previous work has shown that gold nanoparticles (AuNPs) entrapped within amine-terminated generation 5 (G5) PAMAM dendrimers are able to have enhanced interaction with DNA molecules[48,49] and enable enhanced gene delivery applications.[31] This suggests that the entrapment of AuNPs within the dendrimer interior is able to well maintain the 3D conformation of dendrimers, especially when dendrimers are interacted with other biomolecules.

A thorough literature investigation reveals that currently there is no such a report that fully considers the strategies of dendrimer surface PEGylation/ligand modification and internal structural variation for improved gene delivery applications, especially in stem cell gene therapy applications. In this present study, we designed a unique gene delivery system based on dendrimer-entrapped AuNPs (Au DENPs) modified with both PEG monomethyl ether (*m*PEG) and PEGylated RGD (PEG-RGD) (Scheme 1). The formation of the dendrimers and Au DENPs and the ability of the respective vector to compact DNA were characterized via different techniques. The cytotoxicity of these vectors and their polyplexes with pDNA was assessed via cell viability assay. The expression of the enhanced green fluorescent protein and the luciferase (pEGFPLuc) reporter genes was used to evaluate the transfection efficiency of all the synthesized vectors. Finally, the therapeutic potential of the multifunctional RGD-modified Au DENPs as a gene delivery vector was investigated by testing their ability to transfect hMSCs with the human bone morphogenetic protein-2 (hBMP-2) gene and subsequently induce cell differentiation to the osteoblast phenotype. To our knowledge, this is the first report addressing the impact of both the dendrimer surface and internal structural modifications on the performance of stem cell gene delivery.

Scheme 1. Synthesis of (a) G5.NH_2-*m*PEG_{20} Dendrimers (K1), (b) {$(Au^0)_{25}$-G5.NH_2-*m*PEG_{20}} DENPs (K2), (c) G5.NH_2-$(PEG\text{-}RGD)_{10}$-*m*PEG_{10} Dendrimers (K3), and (d) {$(Au^0)_{25}$-G5.NH_2-$(PEG\text{-}RGD)_{10}$-*m*PEG_{10}} DENPs (K4)

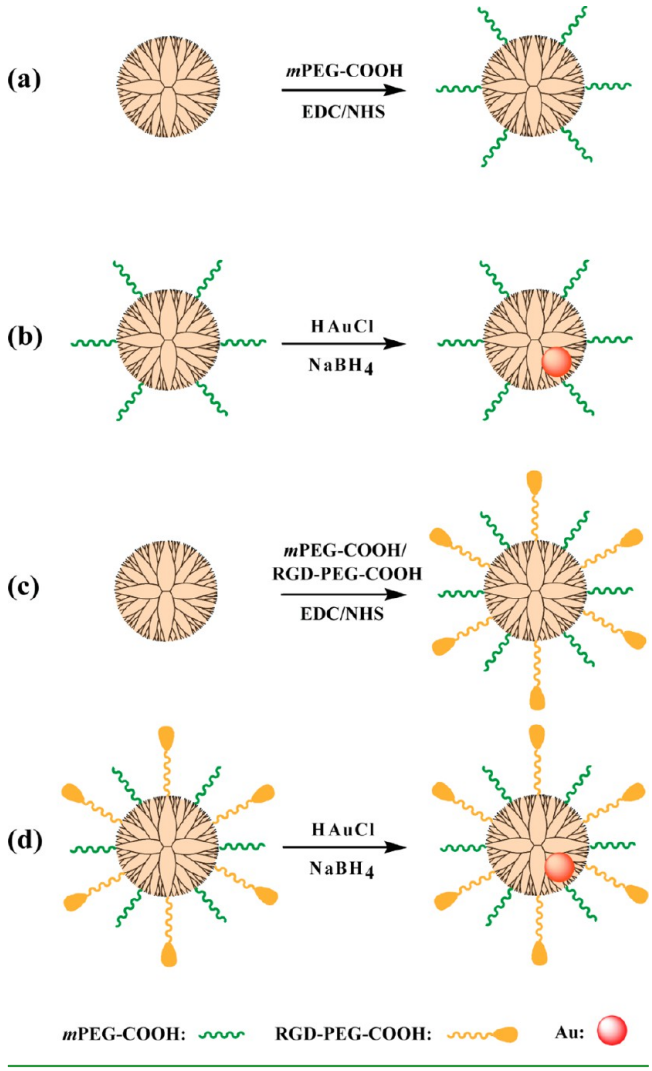

EXPERIMENTAL SECTION

Materials. G5 PAMAM dendrimers were purchased from Dendritech (Midland, MI). PEG with one end of amine group and the other end of carboxyl group (COOH-PEG-NH_2, Mw = 2000) and PEG monomethyl ether with the other end of carboxyl group (*m*PEG-COOH, Mw = 2000) were purchased from Shanghai Yanyi Biotechnology Corporation (Shanghai, China). The pDNA encoding for pEGFPLuc (6.4 kb) was provided by Prof. Tatiana Segura (University of California, Los Angeles, CA), while the pDNA encoding for hBMP-2 (8.5 kb) was kindly donated by Prof. Yasuhiko Tabata (University of Kyoto, Japan). Thiazoyl blue tetrazolium bromide (MTT) was from Sigma-Aldrich (St. Louis, MO). α-Minimum Essential Medium (α-MEM), fetal bovine serum (FBS), penicillin, and streptomycin were purchased from Gibco (Carlsbad, CA). The Primary Amino Nitrogen (PANOPA) Assay Kit was purchased from Megazyme (Wicklow, Ireland). Reporter Lysis Buffer was from Promega (Madison, WI). The QuantiChrom Calcium Assay Kit was from Bioassay System (Hayward, CA). The intact human osteocalcin EIT kit was purchased from Biomedical Technologies Inc. (Stoughton, MA). hMSCs were obtained from the bone marrow of healthy adults after surgical intervention with the approval of the ethical committee of Hospital Dr. Nélio Mendonça, Funchal, Madeira, Portugal. The *p*-nitrophenyl and *p*-nitrophenol standards were from Sigma-Aldrich (St. Louis, MO), and unless otherwise stated, all chemicals with reagent grade were purchased from Sigma-Aldrich and used as received. Water used in all experiments was purified using a Milli-Q Plus 185 water purification system (Millipore, Bedford, MA) with resistivity higher than 18.2 MΩ·cm. Regenerated cellulose dialysis membranes with a molecular weight cutoff (MWCO) of 14 000 were acquired from Fisher Scientific (Pittsburgh, PA).

DOI: 10.1021/am508760w
ACS Appl. Mater. Interfaces 2015, 7, 4833−4843

Synthesis and Characterization of RGD Peptide-Modified Au DENPs. Synthesis of G5.NH_2-*m*PEG_{20} Conjugates. *m*PEG-COOH (23.16 mg, 11.6 mmol), 1-(3-(dimethylamino)propyl)-3-ethylcarbodiimide hydrochloride (EDC, 4.0 mg, 20.88 mmol), and *N*-hydroxysuccinimide (NHS, 2.4 mg, 20.88 mmol) were codissolved in dimethyl sulfoxide (DMSO, 5 mL), and the reaction mixture was stirred for 3 h at room temperature. The activated *m*PEG-COOH was then dropwise added to a solution of G5.NH_2 (15.06 mg, 0.58 mmol) dissolved in DMSO (5 mL) under vigorous magnetic stirring, and the reaction mixture was left for 24 h to obtain the raw product of G5.NH_2-*m*PEG_{20}. The reaction was performed in duplicate.

Synthesis of {$(Au^0)_{25}$-G5.NH_2-*m*PEG_{20}} DENPs. Parallel unpurified G5.NH_2-*m*PEG_{20} dendrimers (obtained from the above duplicated synthesis) were used as templates to synthesize Au DENPs via sodium borohydride reduction chemistry with the molar ratio of gold salt to G5.NH_2-*m*PEG_{20} at 25:1. First, an aqueous solution of $HAuCl_4$ (72.84 mM, 198.67 μL) was dropwise added to an aqueous solution of the G5.NH_2-*m*PEG_{20} dendrimer (0.116 mM, 5 mL) under vigorous magnetic stirring. After 30 min, $NaBH_4$ (72.35 mM, 1 mL) was rapidly added to the gold salt/dendrimer mixture while stirring. The reaction mixture turned to a wine red color within a few seconds. The stirring was continued for 2 h to obtain the raw product of {$(Au^0)_{25}$-G5.NH_2-*m*PEG_{20}} DENPs.

Synthesis of G5.NH_2-(PEG-RGD)$_{10}$-*m*PEG_{10} Conjugates. COOH-PEG-NH_2 (11.58 mg, 5.8 mmol) dissolved in DMSO (5 mL) was dropwise added to a solution of 6-maleimidohexanoic acid N-hydroxysuccinimide ester (6-MAL, 1.785 mg, 5.8 mmol) under vigorous stirring, and the mixture was left for 8 h to obtain the raw product of COOH-PEG-MAL. RGD peptide (4 mg, 0.58 mmol) was then added to the COOH-PEG-MAL solution while stirring. After 12 h, the raw product of the COOH-PEG-RGD conjugate was obtained. EDC (4.0 mg, 20.88 mmol) and NHS (2.4 mg, 20.88 mmol) were added to the COOH-PEG-RGD solution. After this mixture was stirred for 3 h, the activated COOH-PEG-RGD was slowly added to a solution of G5.NH_2 (15.06 mg, 11.6 mmol) dissolved in DMSO (5 mL). The reaction mixture was left under vigorous magnetic stirring for 24 h. Using a dialysis membrane with an MWCO of 14 000, the mixture was then dialyzed against water (nine times, 4 L) for 3 days to remove any excess reactants and byproducts. This was followed by lyophilization to obtain the G5.NH_2-$(PEG\text{-}RGD)_{10}$ product.

Finally, *m*PEG-COOH (11.58 mg, 5.8 mmol) activated according to the protocols described above was added dropwise to a solution of the G5.NH_2-$(PEG\text{-}RGD)_{10}$ dendrimer dissolved in DMSO (5 mL). This reaction was continued for 24 h under vigorous magnetic stirring to obtain the raw product of the G5.NH_2-$(PEG\text{-}RGD)_{10}$-*m*PEG_{10} conjugates. The reaction was performed in duplicate.

Synthesis of {$(Au^0)_{25}$-G5.NH_2-$(PEG\text{-}RGD)_{10}$-*m*PEG_{10}} DENPs. Parallel unpurified G5.NH_2-$(PEG\text{-}RGD)_{10}$-*m*PEG_{10} conjugates (obtained from the above duplicated synthesis) were used as templates to synthesize the {$(Au^0)_{25}$-G5.NH_2-$(PEG\text{-}RGD)_{10}$-*m*PEG_{10}} DENPs with the molar ratio of Au salt/dendrimer at 25:1 according to the procedures described above.

All the raw products mentioned above were purified by dialysis against water (nine times, 4 L) for 3 days to remove the excess reactants using a dialysis membrane with MWCO of 14 000. This was followed by lyophilization to obtain the final products. For simplicity, G5.NH_2-*m*PEG_{20}, {$(Au^0)_{25}$-G5.NH_2-*m*PEG_{20}}, G5.NH_2-$(PEG\text{-}RGD)_{10}$-*m*PEG_{10}, and {$(Au^0)_{25}$-G5.NH_2-$(PEG\text{-}RGD)_{10}$-*m*PEG_{10}} were denoted as K1, K2, K3, and K4, respectively, in our naming system. The pristine G5.NH_2 dendrimer was denoted as K0.

Characterization Techniques. ^1H NMR spectra were collected using a Bruker AV400 NMR spectrometer. All dendrimers or DENPs were dissolved in D_2O before measurements. UV−vis spectra were recorded using a Lambda 25 UV−vis spectrophotometer (PerkinElmer, Boston, MA). All samples were dissolved in water before measurements. TEM was performed using a JEOL 2010F analytical electron microscope (JEOL, Tokyo, Japan) with an accelerating voltage of 200 kV. TEM samples were prepared by depositing an aqueous suspension of Au DENPs (5 μL, 2 mg/mL) onto a carbon-coated copper grid and air-dried before observation. ImageJ software (http://rsb.info.nih.gov/ij/download.html) was used to analyze the size and size distribution of each sample. At least 200 NPs randomly selected from different TEM images were measured for each sample. To determine the number of the terminal primary amine groups present on the surface of dendrimers or Au DENPs, Megazyme's PANOPA Assay Kit was used and the assays were performed according to the manufacturer's instructions.

Polyplex Preparation. Each vector/pDNA polyplex was prepared, taking into account the ratio of the number of primary amines on the vector surface to the number of phosphate groups in the pDNA backbone (i.e., the N/P ratio). To prepare the polyplexes, both vector and pDNA solutions were diluted with phosphate buffer saline (PBS, pH 7.4) at different N/P ratios. In each case, 1 μg pDNA was used. The mixtures were gently vortexed and incubated at room temperature for 30 min before characterization or transfection.

Gel Retardation Assay. To confirm the vector/pDNA polyplex formation, an agarose gel retardation assay was performed. Each vector/pDNA polyplex was prepared by mixing 1 μg of pDNA (pEGFPLuc) and the corresponding vector in PBS (pH 7.4). A 1% (w/v) agarose gel containing 0.1 μg/mL ethidium bromide (EB) was prepared using Tris-acetate-EDTA buffer. Gel electrophoresis was carried out at 80 V for 30 min. The retardation of the pDNA was visualized using a gel image analysis system (Shanghai FURI Science & Technology, Shanghai, China).

Dynamic Light Scattering and Zeta Potential Measurements. Each vector/pDNA (hBMP-2) polyplex at an N/P ratio of 1:1, 2.5:1, or 5:1 was diluted by PBS to have a final volume of 1 mL. Here 5 μg of pDNA was used to form the polyplex. Dynamic light scattering (DLS) and zeta potential measurements were performed using a Zetasizer Nano-ZS (Malvern Instruments, UK) equipped with a standard 633 nm laser to measure the hydrodynamic sizes and surface potentials of the vector/pDNA polyplexes.

Scanning Electron Microscopy (SEM) Observation. We selected K2 and K4 vectors to prepare vector/pDNA (hBMP-2) polyplexes at an N/P ratio of 2.5:1. The vector/pDNA polyplexes were prepared according to the above protocols (except that water was used) and diluted by water to achieve a final volume of 1 mL. SEM was performed using a TM-100 scanning electron microscope (Hitachi, Tokyo, Japan) with an operating voltage of 5 kV. Before measurement, the samples dispersed in water were dropped onto aluminum foil, air-dried, and sputter-coated with a 5-nm-thick Au film.

Cytotoxicity Assay. The cytotoxicity of the vectors or vector/pDNA (hBMP-2) polyplexes was assessed by the MTT viability assay of the hMSCs. In brief, 1.5×10^4 cells were seeded into each well of 96-well plates with 100 μL of α-MEM containing 10% FBS, 100 U/mL penicillin, and 100 U/mL streptomycin at 37 °C and 5% CO_2 the day before the experiments. On the next day, the medium was replaced with fresh α-MEM containing vectors (10 μL in PBS) with a dendrimer molar concentration ranging from 50 to 3000 nM. Cells treated with PBS were used as control. After incubation of the cells at 37 °C for 24 h, the medium in each well was replaced with fresh α-MEM containing MTT (5.0 mg/mL, 20 μL in PBS). The cells were incubated for another 4 h at 37 °C. Finally, the medium within each well was replaced with 150 μL of DMSO to dissolve the formed formazan crystals. After the plates were shaken for 15 min, the absorbance at a wavelength of 490 nm was measured using a PerkinElmer microplate reader (Victor^3 1420, Boston, MA). The reference wavelength was set at 630 nm. The cytotoxicity of the vector/pDNA polyplexes was also tested via the MTT assay. The molar concentration of the vectors ranged from 50 to 3000 nM, and the dose of pDNA used for each well was 1 μg. The experiment was carried out as described above.

Transfection Assays Using the Luc and EGFP Genes. hMSCs were seeded in 24-well plates at a density of 1.5×10^4 cells/well and cultivated for 24 h at 37 °C and 5% CO_2 until a cell confluency of 60−70% was obtained. Subsequently, the medium in each well was replaced by 500 μL of polyplex-containing serum-free fresh medium. All polyplex solutions were prepared at N/P ratios of 1:1, 2.5:1, and 5:1, respectively, using 1 μg of pDNA. Nontransfected cells and cells transfected with naked pDNA were used as negative controls. After

DOI: 10.1021/am508760w
ACS Appl. Mater. Interfaces 2015, 7, 4833−4843

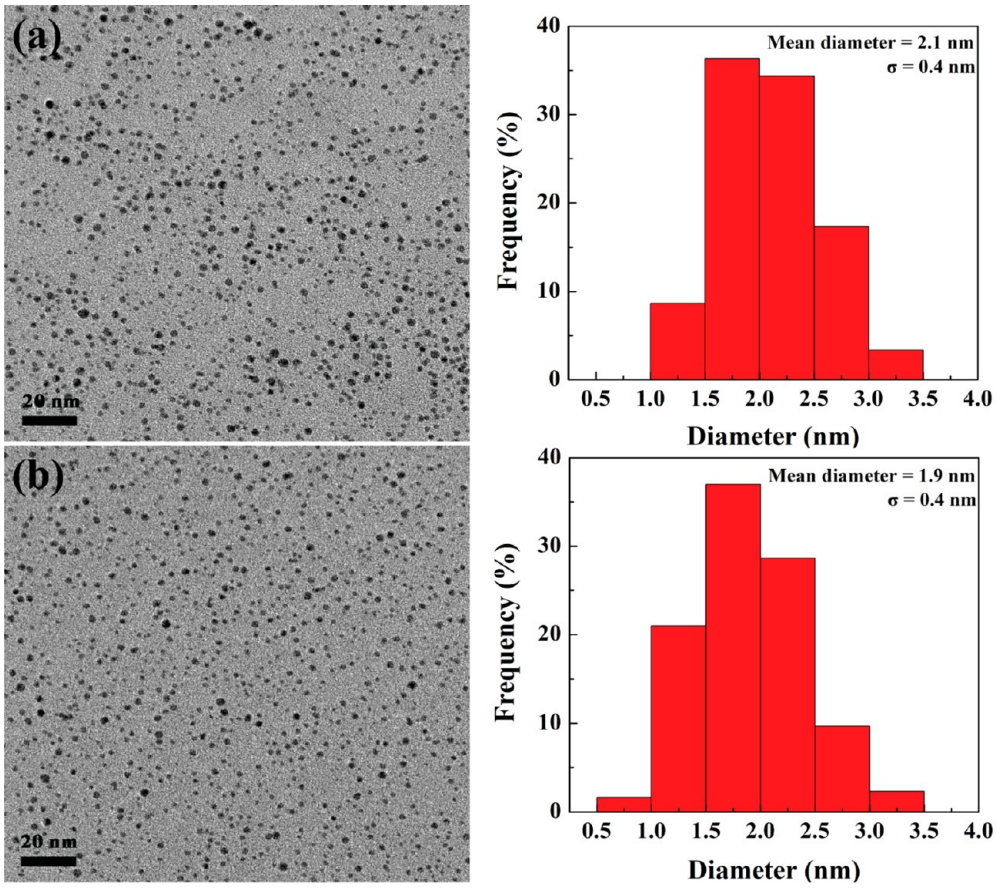

Figure 1. TEM image and size distribution histogram of (a) $\{(Au^0)_{25}$-G5.NH_2-mPEG$_{20}\}$ (K2) and (b) $\{(Au^0)_{25}$-G5.NH_2-(PEG-RGD)$_{10}$-mPEG$_{10}\}$ (K4) DENPs.

incubation of the cells for 4 h, the medium in each well was replaced by fresh complete medium containing 10% FBS, and the cells were further incubated for 24 h. Then the medium was removed, and the cells were washed three times with 1 mL of PBS. The Luc activity of the harvested cells was analyzed using the Luc Assay Kit (Promega) according to the manufacturer's instructions. Luc expression was used to calculate the gene delivery efficiency of each vector and was recorded as relative light units per milligram of total protein (RLU/mg).

The ability of the vectors to efficiently deliver exogenous genes was also evaluated by monitoring the expression of the EGFP gene. Here the hMSCs were transfected with the vector/pDNA polyplexes at an N/P ratio of 2.5:1 under the experimental conditions described above. The cells were observed and imaged 24 h post-transfection using fluorescence microscopy (Nikon Eclipse TE 2000E inverted microscope). The fluorescence intensity of each image was quantified via ImageJ software (see above for more information).

Transfection Assay Using the hBMP-2 Gene. For transfection using the hBMP-2 gene-carrying plasmid DNA, hMSCs (1.5×10^4 cells/well) were plated in 24-well plates and cultured under 37 °C and 5% CO_2 for 24 h. The cells were then transfected with vector/pDNA polyplexes prepared at an N/P ratio of 2.5:1 using a fixed dose of 1 μg/well of the hBMP-2 plasmid. After 4 h, the medium within each well was removed and replaced by complete medium containing 10% FBS, 100 U/mL penicillin, 100 U/mL streptomycin, 50 μg/mL ascorbic acid, and 5 nM β-glycerophosphate. After 3 days, 100 μL of the supernatant was collected, and the expression level of the hBMP-2 gene was then analyzed using a human BMP-2 ELISA Kit (Antigenix America Inc., Stoughton, MA).

Evaluation of Osteogenic Differentiation of hMSCs. ALP Activity Assay. hMSCs were plated at 1.5×10^4 cells/well in 24-well plates with 1 mL of α-MEM containing 10% FBS, 100 U/mL penicillin, 100 U/mL streptomycin, 50 μg/mL ascorbic acid, and 5 nM β-glycerophosphate. On days 7, 14, and 21, the ALP activity of the hMSCs was quantified using a colorimetric assay in which the hydrolysis of p-nitrophenyl phosphate to p-nitrophenol was monitored. Briefly, the cell culture medium within each well was removed, and the cells were rinsed three times with PBS. Reporter lysis buffer (400 μL) was then added to each well, and the cell lysis was carried out according to the manufacturer's instruction. The cell lysate (20 μL) was then transferred to a corresponding well of a 96-well plate. To each well was then added 200 μL of the ALP substrate. After incubation of the samples in the dark for 1 h at 37 °C, 10 μL of 0.02 M NaOH was added to stop the reaction. Finally, the absorbance at 405 nm was read using a PerkinElmer Victor^3 1420 microplate reader. The ALP activity of the hMSCs under various conditions was then quantified using a standard curve which was prepared using serial dilutions of p-nitrophenol.

Osteocalcin Secretion Assay. Cells were grown in cell culture medium as described above for the osteocalcin secretion assay and the following other assays. Medium of each well was collected on days 14 and 21, and the osteocalcin secreted to the culture medium was measured using an intact human osteocalcin ELISA kit (Biomedical Technologies Inc., Boston, MA). Twenty-four hours prior to sample collection, the medium was replaced with fresh serum-free medium. The obtained medium was then analyzed in triplicate according to the manufacturer's recommendations.

Calcium Deposition Assay. Deposited calcium in culture was measured using the QuantiChrom Calcium Assay Kit (DICA-500). Here hMSCs were harvested from complete medium on days 14 and 21. After lysis, aliquots of 5 μL of the cell lysates were transferred to each respective well of a 96-well plate. After the addition of 200 μL of working reagent to each respective well, the plates were gently tapped to mix the samples. The plates were then incubated at room temperature for 3 min, after which the optical density at 612 nm was

DOI: 10.1021/am508760w
ACS Appl. Mater. Interfaces 2015, 7, 4833−4843

recorded using a PerkinElmer Victor^3 1420 microplate reader. A standard curve generated using serial dilutions of $CaCl_2$ was used to calculate the final concentration of Ca^{2+} in the samples.

Von Kossa Staining. Von Kossa staining was used to qualitatively assess the mineralization degree achieved by cells in culture. Briefly, the culture plates were taken out on day 21. After discarding the culture medium, the cells were rinsed three times with PBS and then fixed with 3.7% formaldehyde solution for 15 min at room temperature. After removing the solution, the samples were rinsed with water several times. The cells were subsequently treated with 2.5% silver nitrate solution and exposed to ultraviolet light for 60 min. At this stage, the plates were washed with water and then treated with 5% sodium thiosulfate solution for 3 min. Finally, after washing with water, the plates were examined using a Nikon Eclipse TE 2000E inverted microscope.

Statistical Analysis. The one-way ANOVA method was used to assess the statistical differences of the experimental data. Results are reported as mean ± standard deviation. A p value of 0.05 was selected as the significance level, and the data were labeled as follows: (*) for $p < 0.05$, (**) for $p < 0.01$, (***) for $p < 0.001$, respectively.

RESULTS AND DISCUSSION

Synthesis and Characterization of RGD Peptide-Modified Au DENPs. According to the protocols described in our previous study related to the preparation of PEGylated dendrimers[13,15,16,36] and the formation of Au DENPs,[31,50] we prepared K1, K2, K3, and K4 vectors, respectively (Scheme 1). The selection of both *m*PEG-COOH and COOH-PEG-NH_2 with an Mw of 2000 is based on our previous work,[15,16] where PEGylation of G5 dendrimers enables enhanced loading of Au content and significantly improved cytocompatibility. Likewise, the linking of RGD peptide to the dendrimer surface via a PEG spacer is believed to be able to render each vector with minimal protein adsorption,[51] thereby avoiding the protein corona-induced nonspecificity. The conjugation of *m*PEG and PEG-RGD to the amine-terminated G5.NH_2 dendrimers was first characterized by ^{1}H NMR (Figure S1, Supporting Information). The methylene protons of PEG at 3.60 ppm (Figure S1a), the RGD-associated aromatic proton peaks at 7.3 and 7.4 ppm (Figure S1b), and the methylene protons of PAMAM dendrimers in the range of 2.2−3.4 ppm can be easily identified, confirming the successful conjugation of *m*PEG and PEG-RGD onto the G5 dendrimer surface. Through NMR peak integration, the number of *m*PEG (for K1) conjugated onto each dendrimer was calculated to be 19.9, which is approximately similar to the initial molar feeding ratio of *m*PEG/dendrimer. Likewise, for the K3 dendrimer, the numbers of the total PEG and RGD moieties conjugated onto each dendrimer molecule were calculated to be 19.0 and 9.0, respectively.

The synthesized K1 and K3 dendrimers were then used as templates to synthesize K2 and K4 DENPs, respectively. UV−vis spectroscopy was used to verify the formation of Au DENPs (Figure S2, Supporting Information). An absorption peak at around 510 nm in the spectra of both K2 and K4 can be attributed to the typical surface plasmon band of AuNPs, thereby confirming the successful synthesis of the respective Au DENPs.

TEM was used to examine the shape and size distribution of the Au core NPs in the two different Au DENPs (Figure 1). It can be seen that both Au DENPs display a quite spherical shape with a narrow size distribution. The average size of the Au core NPs for K2 (Figure 1a) and K4 (Figure 1b) was estimated to be 2.1 and 1.9 nm, respectively. Our results suggest that the RGD modification onto the surface of dendrimers does not appreciably affect the shape and size distribution of the Au core NPs. The hydrodynamic size of each vector was analyzed by DLS, and the results are shown in Table S1 (Supporting Information). It can be seen that the modification of G5.NH_2 dendrimers with *m*PEG, *m*PEG + AuNPs, *m*PEG + RGD, *m*PEG + AuNPs + RGD does not significantly alter the hydrodynamic size of the pristine G5.NH_2 dendrimer.

To accurately prepare the different vector/pDNA polyplexes using the selected N/P ratios, measurement of the number of primary amines on the vector surface is indispensable. Table 1 shows the mean number of primary amines on the vector surfaces determined using the PANOPA assay. We show that there are 98.0 primary amines on the K0 surface, while the number of primary amines on the surface of the other vectors is lower than that of K0 and follows the order of K1 > K3 > K2 > K4. This can be attributed to the replacement of some of the primary amines on the G5.NH_2 dendrimer surface with *m*PEG and PEG-RGD. Likewise, the entrapment of AuNPs requires more dendrimer primary amines to be used to stabilize them; therefore, the number of primary amines for K2 and K4 is lower than that for the corresponding templates K1 and K3, respectively, in agreement with our previous work.[31]

Table 1. Physicochemical Parameters of the Formed Vectors

vector	K0	K1	K2	K3	K4
Mw[a]	26010	66010	70900	72920	77810
mean number of primary amines per dendrimer	98.0	75.3	44.9	61.9	39.7

[a]Calculated based on the practical Mw of K0.

Gel Retardation Assay. Cationic polymer vectors are able to compact negatively charged pDNA via electrostatic interaction.[31] To evaluate the ability of different vectors to condense pDNA at different N/P ratios, agarose gel retardation assay was performed (Figure 2). It can be seen that the mobility of the pDNA can be retarded by all the different vectors at an N/P ratio of 1:1 or above, indicating that the developed dendrimer-based vectors with or without AuNPs are efficient in compacting pDNA at an N/P ratio of 1:1 or greater. Therefore, N/P ratios of 1:1 or above were selected for the following studies. Our results suggest that the partial PEGylation or RGD modification of the surface of G5 dendrimers and the subsequent entrapment of AuNPs within the respective G5 dendrimers do not appreciably affect the DNA compaction capability when compared with the pristine K0 vector.

Hydrodynamic Diameter and Zeta Potential Measurements. To efficiently transport exogenous genes to the cell nucleus, the designed vector/pDNA polyplex should have an appropriate size and relative positive surface potential. As shown in Figure 3a, all vector/pDNA polyplexes with an N/P ratio of 1:1, 2.5:1, or 5:1 displayed a hydrodynamic diameter in a range of 118−201 nm (polydispersity index (PDI) data are shown in Table S2, Supporting Information). The hydrodynamic diameter appears to decrease with the increase of the N/P ratio. To confirm the DLS results, we used SEM to observe the size of the two representative K2/pDNA and K4/pDNA polyplexes formed at an N/P ratio of 2.5 (Figure S3, Supporting Information). Clearly, the polyplexes are aggregated together due to the sample drying effect.[52] The size of the K2/pDNA and K4/pDNA polyplexes was measured to be 161.4 ± 4.4 nm and 210.4 ± 4.3 nm, respectively, quite similar to the DLS data. Similarly, zeta potential measurements show that at

DOI: 10.1021/am508760w
ACS Appl. Mater. Interfaces 2015, 7, 4833−4843

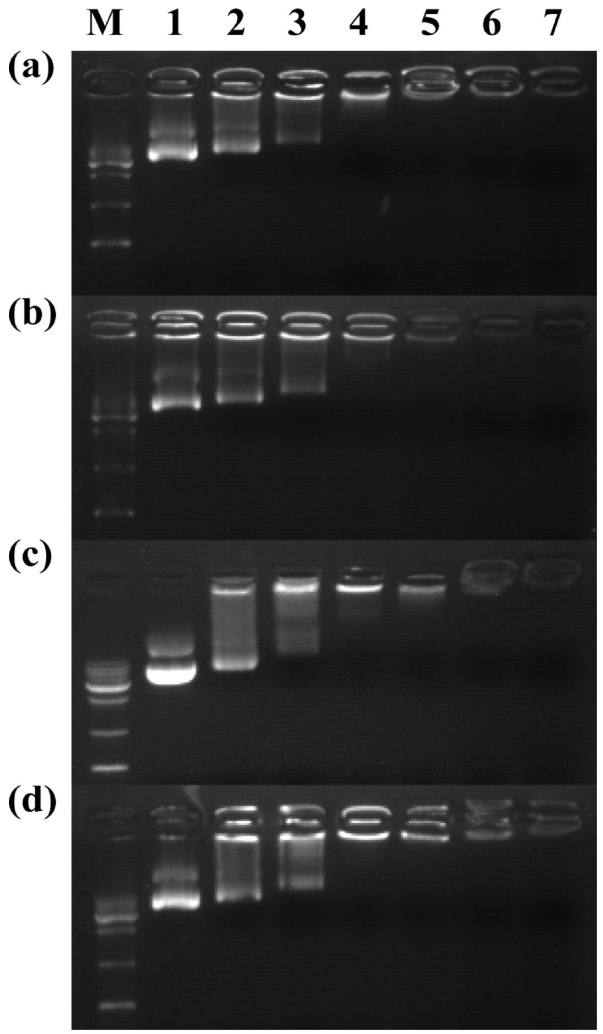

Figure 2. Gel retardation assay of K1/pDNA (a), K2/pDNA (b), K3/pDNA (c), and K4/pDNA (d) polyplexes at different N/P ratios. Lane M: marker; lane 1: N/P = 0.125:1; lane 2: N/P = 0.25:1; lane 3: N/P = 0.5:1; lane 4: N/P = 1:1; lane 5: N/P = 2:1; lane 6: N/P = 3:1; lane 7: N/P = 4:1.

similar N/P ratios, the modification of *m*PEG or PEG-RGD on the G5 dendrimer surface and the subsequent entrapment of AuNPs do not seem to significantly impact the surface potential of the polyplexes when compared to the K0/pDNA polyplexes (Figure 3b). At the N/P ratios of 2.5:1 and 5:1, all polyplexes display a surface potential in a range of 14.7−22.0 mV. Combining the hydrodynamic size and surface potential data reveals that the modification of G5 dendrimers either via surface modification with *m*PEG/PEG-RGD or via subsequent entrapment of AuNPs renders the formed vector/pDNA polyplexes with quite small hydrodynamic size and relatively positive surface potential, which are suitable for further gene delivery applications.

Cytotoxicity Assay. For gene delivery applications, it is prerequisite to first explore the cytocompatibility of the vector or vector/pDNA polyplexes (Figure 4). For hMSCs treated with K0, K1, K2, K3, and K4 vectors, the cell viability was observed to gradually decrease with an increase of the vector concentration (Figure 4a). This is consistent with the data reported in our previous work.[31] Under similar dendrimer concentrations (500 nM or above), it seems that modified dendrimers and the respective Au DENPs are less cytotoxic than the pristine K0 dendrimer. This could be due to the fact that the amine density of the G5 dendrimers is significantly reduced after dendrimer modification via either surface functionalization or entrapment of AuNPs. Similarly, for hMSCs treated with different vector/pDNA polyplexes (Figure 4b), the cell viability decreased with the increase of dendrimer concentration, and the polyplexes formed using the modified dendrimers or Au DENPs were less cytotoxic than the K0/pDNA polyplex under similar dendrimer concentrations. Importantly, under the same dendrimer concentrations, the cytotoxicity of each vector/pDNA polyplex was much less than that of the respective vector. This should be due to the fact that the complexation of pDNA further decreases the amine density of the dendrimer-based vectors, thereby alleviating the electrostatic interaction-induced cytotoxicity.[53] Overall, our data show that the modification of G5.NH_2 dendrimers via surface PEGylation or interior AuNP entrapment is beneficial to improve the cytocompatibility of the dendrimer-based vectors, which is beneficial for safe gene delivery applications.

Gene Transfection Efficiency. To investigate the transfection efficiency of each dendrimer-based nonviral vector, a pDNA carrying the EGFP and the Luc reporter genes was used. Figure 5 shows that the K1/pDNA, K2/pDNA, K3/pDNA, and K4/pDNA polyplexes exhibit distinctly higher Luc activity relative to the K0/pDNA polyplex at N/P ratios of 1:1 and 2.5:1. At the tested highest N/P ratio of 5:1, it seems that the cells transfected with the K0/pDNA polyplex have the highest Luc activity. However, polyplexes with a high N/P ratio also have a higher cytotoxicity (Figure 4b). In this context, the modification of the dendrimer vector enables highly efficient

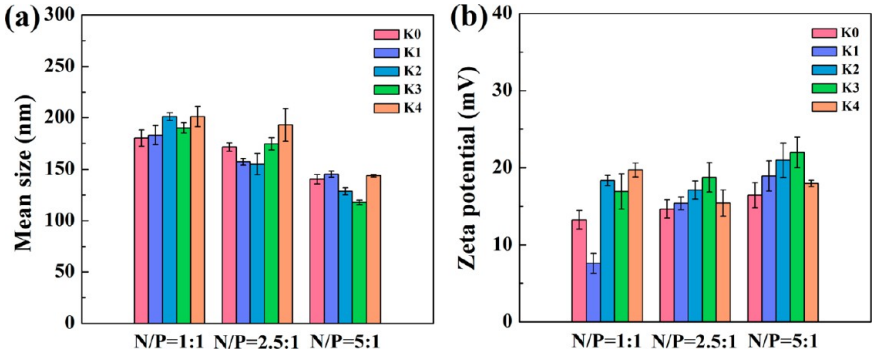

Figure 3. Mean hydrodynamic size (a) and surface potential (b) of different vector/pDNA polyplexes under different N/P ratios (mean ± SD, n = 3).

DOI: 10.1021/am508760w
ACS Appl. Mater. Interfaces 2015, 7, 4833−4843

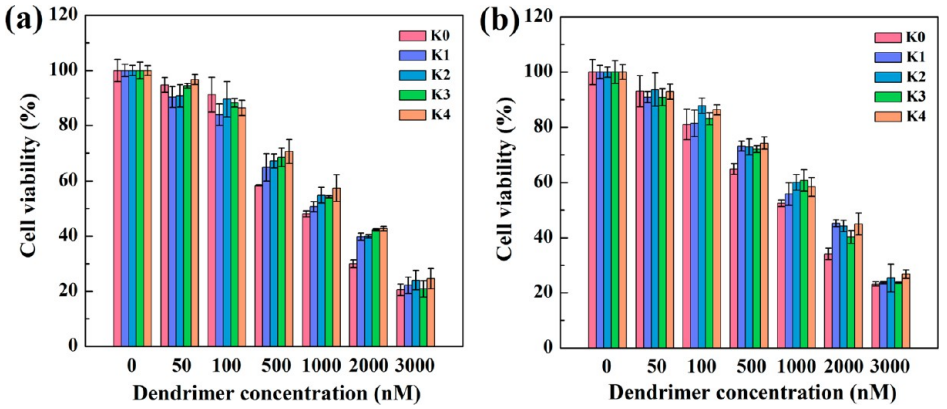

Figure 4. MTT viability assay of hMSCs treated with different vectors (a) and vector/pDNA polyplexes (b) at different dendrimer concentrations (mean ± SD, n = 3). The results are presented as the percentage of viable cells in relation to the control cells treated with PBS.

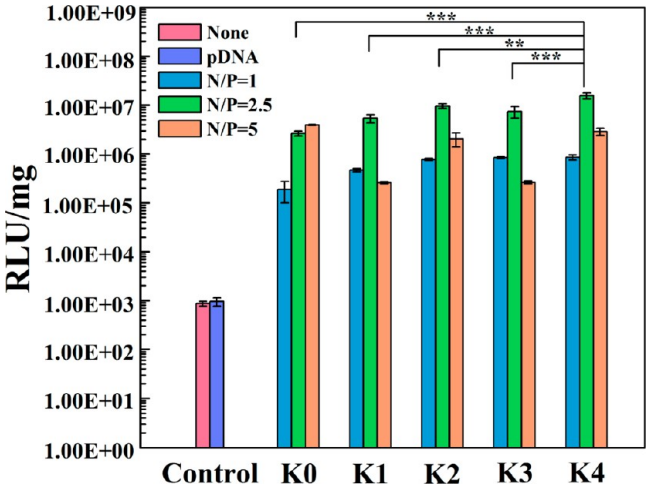

Figure 5. Luciferase gene transfection efficiency of vector/pDNA polyplexes in hMSCs at N/P ratios of 1:1, 2.5:1, 5:1, respectively (mean ± SD, n = 3). Nontransfected cells and cells treated with free pDNA were used as controls.

gene delivery at a low N/P ratio, which is beneficial for safe gene delivery applications. At an N/P ratio of 2.5:1, the K4 vector has the highest gene transfection efficiency when compared with the other four vectors (p < 0.01), and the Luc activity of cells follows the order of K4 > K2 > K3 > K1 > K0. Interestingly, the above results suggest that the modification of G5.NH_2 with *m*PEG alone improves gene transfection efficiency, and also that modification with RGD via PEG spacers further enhances the gene delivery. This is due to the fact that partial PEGylation of the dendrimers increases the solubility of the vector/pDNA polyplexes and enhances the intracellular release of DNA molecules,[29,54] in agreement with the literature.[38] Likewise, the hMSCs are known to express integrins that can recognize the attached RGD peptide via ligand−receptor interaction,[45] enhancing the intracellular uptake of the polyplexes not only through electrostatic interaction but also through a receptor-mediated pathway. In addition to this, the entrapment of AuNPs within the respective *m*PEG-modified and PEG-RGD-modified dendrimers further improves the gene transfection efficiency due to the preservation of the 3D shape of dendrimers, which is helpful to enhance the interaction between the vectors and pDNA, in agreement with the literature.[31] Overall, by comparison of the K0 vector in the case of N/P = 2.5, the gene delivery efficiency using K1 (*m*PEG modification), K2 (*m*PEG + AuNPs modification), K3 (*m*PEG + RGD modification), and K4 (*m*PEG + AuNPs + RGD modification) was enhanced by 104%, 264%, 180%, and 495%, respectively. This clearly suggests that the modification of AuNPs/RGD peptides or both of them is able to significantly improve the gene delivery efficiency.

To further confirm the effective gene transfection efficacy of the different dendrimer-based vectors, fluorescence microscopy was used to visualize the EGFP expression in the hMSCs. Here the optimal conditions for gene transfection were selected by taking into account the maximum RLU values measured for all the vectors in the Luc gene expression studies. On this basis, fluorescence microscopy images of EGFP expression in the hMSCs were acquired following the treatment of the cells with polyplexes prepared at an N/P ratio of 2.5:1 (Figure 6). In accordance with the quantitative analysis of the Luc activity, the green fluorescent signals arising from the EGFP expression are observed. In particular, PEG- and PEG-RGD-modifications of the G5.NH_2 dendrimer, as well as the entrapment of AuNPs within the respective dendrimers, play a key role in enhancing the gene transfection efficiency. The EGFP gene expression was quantified by measuring the fluorescence intensity of the cells in each image using ImageJ software (Table S3, Supporting Information). It can be seen that the EGFP gene expression follows the order of K4 > K2 > K3 > K1 > K0, in agreement with the Luc activity assay. It should be noted that through the combination of the quantitative Luc activity assay and qualitative fluorescence microscopic observation of EGFP expression, the gene transfection efficiency of the dendrimeric vectors are able to be sufficiently verified, in agreement with the literature.[31,55,56]

Transfection Assays Using hBMP-2 Gene. On the basis of the transfection performance of pEGFPLuc using different dendrimer-based vectors, we selected an N/P ratio of 2.5:1 to evaluate the possibility of using the developed vector systems to transfect hMSCs with a pDNA carrying the hBMP-2 reporter gene. From Figure 7a, it is clear that the nontransfected cells do not have appreciable hBMP-2 expression. In contrast, the hBMP-2 protein is expressed in cells transfected with the different dendrimer-based vectors. The hBMP-2 gene transfection efficiency followed the order of K4 > K2 > K3 > K1 > K0, similar to the above Luc gene transfection results. The highest hBMP-2 gene transfection efficiency using the K4 vector should be due to the fact that the PEG-RGD

DOI: 10.1021/am508760w
ACS Appl. Mater. Interfaces 2015, 7, 4833−4843

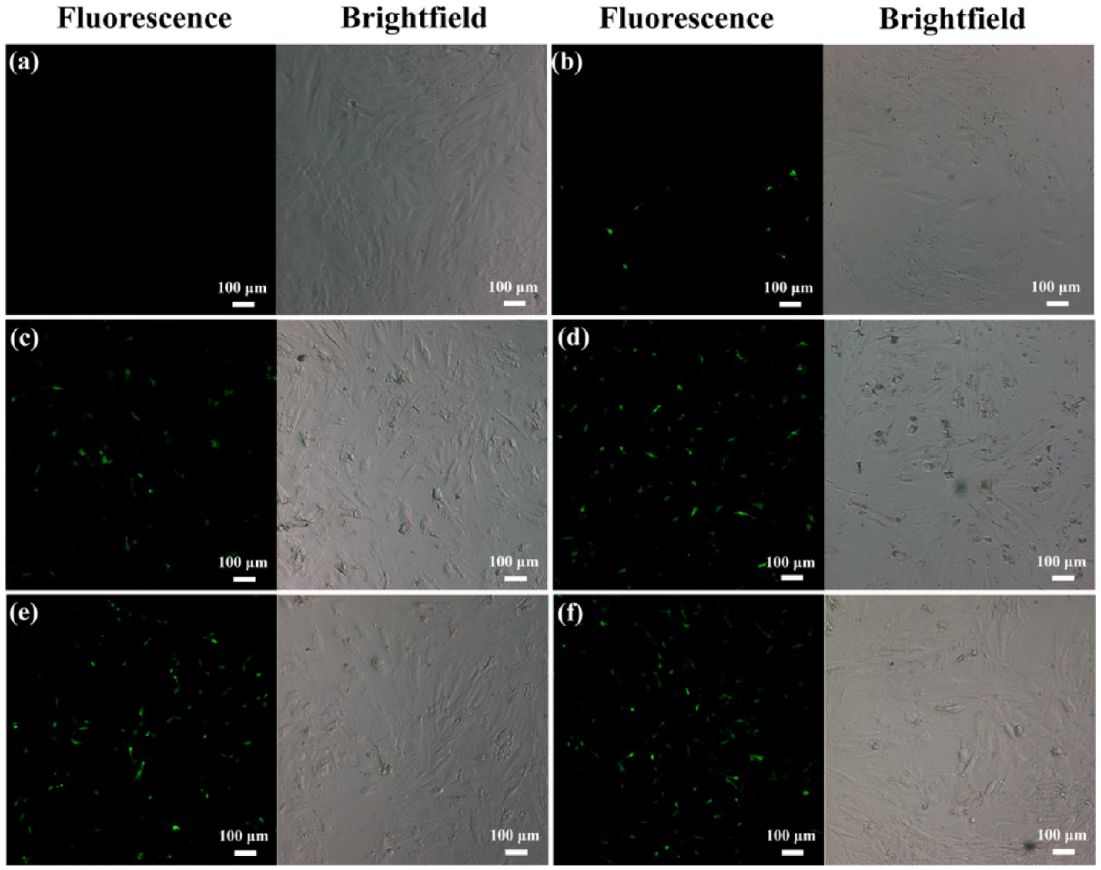

Figure 6. Fluorescence microscopic images of EGFP gene expression in hMSCs using vector/pDNA polyplexes at an N/P ratio of 2.5:1. Images were taken 24 h post-transfection. The cells were transfected with (b) K0/pDNA, (c) K1/pDNA, (d) K2/pDNA, (e) K3/pDNA, and (f) K4/pDNA polyplexes. Nontransfected cells (a) were used as control.

modification of dendrimers and the entrapment of AuNPs within the dendrimers render the vector with RGD-mediated targeting effect and well-maintained 3D conformation of dendrimers, respectively.

To confirm the hBMP-2 gene transfection-induced stem cell osteogenic differentiation, the activity of ALP, which is a membrane-bound enzyme secreted early in bone formation and has been identified to be an important early marker of osteogenesis,[38−40] was analyzed. Figure 7b shows that the ALP activity increases with the cell culture time for hMSCs transfected with a given vector/pDNA complex. Additionally, the ALP activity of hMSCs on day 21 is significantly higher than that on days 7 and 14. At all time points, the ALP activity for the transfected hMSCs is obviously higher than that for the nontransfected cells. Apparently hMSCs transfected using the K4 vector displays the highest ALP activity when compared with the other vectors due to the surface PEG-RGD modification and the entrapped AuNPs.

Osteocalcin is synthesized and secreted by osteoblasts and has been identified as an important marker of late-stage osteogenic differentiation.[57] Both nontransfected and transfected cells displayed a low production rate of osteocalcin on day 14 (Figure 7c). On day 21, a distinct increase in the level of osteocalcin secretion was detected for all transfected hMSCs, suggesting that hMSCs after transfection with the hBMP-2 gene using different dendrimer-based vectors are able to be differentiated into the osteoblast lineage. Also, relative to K0, the K1, K2, K3, and K4 vector-transfected hMSCs were all observed to have visibly higher levels of osteocalcin secretion on day 21. Similarly, the K4 vector enabled the transfected hMSCs to have the highest osteocalcin secretion when compared to all other vectors, corroborating the ALP activity data.

Calcium deposition is another indicator that can be used to further characterize the degree of hMSC osteogenic differentiation (Figure 7d). The results clearly demonstrate higher quantities of calcium production in the transfected hMSCs cultures than in the nontransfected cultures. With time, the deposition of calcium progressively increased from day 14 to day 21, in agreement with work previously reported in the literature.[5] On both day 14 and day 21, hMSCs transfected by the K4 vector displayed the highest calcium content when compared to the other vectors. These results further verify that all dendrimer-based vectors can deliver exogenous genes and successfully induce the hMSC osteogenic differentiation, with K4 being the most effective vector.

To qualitatively characterize the osteogenesis process, Von Kossa staining[8] was used to measure the mineralization of the cell extracellular matrix 21 days post-transfection (Figure 8). The cells were typically stained to be dark, indicating the generation of the calcium phosphate crystals.[5] For nontransfected hMSCs (Figure 8a), the culture is transparent and the cell morphology is obviously different from cells transfected with the different vector/pDNA polyplexes. Analysis of the density of the dark region indicates that hMSCs transfected with the K4 vector display the darkest intensity (Figure 8f). This again confirms that all dendrimer-based vectors are able to transfect the hBMP-2 gene to hMSCs to enable osteogenic

DOI: 10.1021/am508760w
ACS Appl. Mater. Interfaces 2015, 7, 4833−4843

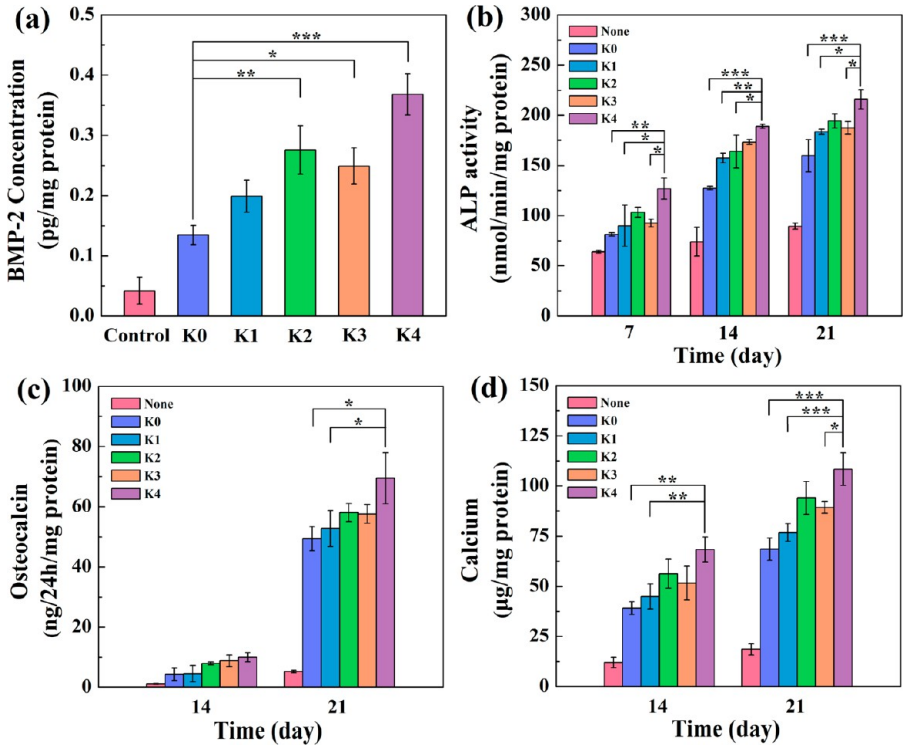

Figure 7. (a) hBMP-2 expression in hMSCs 3 days post-transfection via different vectors. (b) Time course of ALP activity of hMSCs transfected with different vector/pDNA polyplexes. (c) Osteocalcin content secreted by hMSCs transfected with different vector/pDNA polyplexes at different culture times. (d) Calcium deposition on the extracellular matrix of the hMSCs transfected with different vector/pDNA polyplexes after being cultured for 14 and 21 days. All data were presented as mean ± SD (n = 3). Nontransfected cells were used as control.

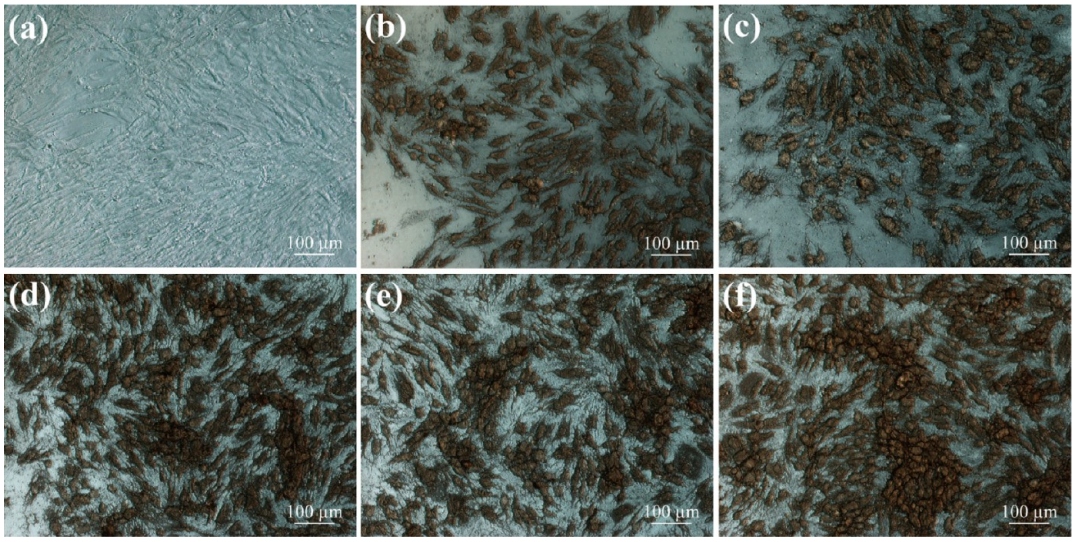

Figure 8. Von Kossa staining of hMSCs transfected with K0/pDNA (b), K1/pDNA (c), K2/pDNA (d), K3/pDNA (e), and K4/pDNA (f) polyplexes on day 21. Nontransfected cells (a) were used as control.

differentiation of the hMSCs. The K4 vector possessing both PEG-RGD and AuNPs displays the best gene transfection efficiency.

CONCLUSION

In summary, we developed functionalized dendrimers and Au DENPs as vectors for gene delivery to stem cells. Our study clearly shows that hMSCs can be transfected with two different pDNAs (encoding EGFP/Luc and hBMP-2 genes) at an N/P ratio of 2.5:1. In particular, the hBMP-2 gene transfection enables the hMSCs to be differentiated into the osteoblastic lineage. Our results suggest that the gene delivery efficiency is largely dependent on the composition and surface modification of the vector. The surface modification with PEG-RGD and the entrapment of AuNPs render the dendrimer platform not only with targeting specificity to recognize integrin-expressing hMSCs but also with the well-maintained 3D conformation to have improved DNA compaction ability, thus affording the dendrimer-based vector with high gene transfection efficiency and specificity. In addition, the role played by the entrapped

DOI: 10.1021/am508760w
ACS Appl. Mater. Interfaces 2015, 7, 4833−4843

AuNPs within the dendrimer interior should be multiple: (1) reducing dendrimer amine functionality by counter charge to improve the biocompatibility of the vectors; (2) possibly enabling the vector with X-ray imaging functionality[16] and photothermal therapy potency.[58,59] The developed RGD-functionalized Au DENPs may provide a basis for rational design of functional nonviral vectors for enhanced gene delivery applications and may hold great promise to be used in the field of tissue engineering, regenerative medicine, and cancer theranostic nanomedicine.

■ ASSOCIATED CONTENT

Supporting Information

Additional experimental data including DLS of vector and vector/pDNA polyplexes, ^{1}H NMR and UV−vis spectroscopic data of functionalized dendrimers and Au DENPs, and SEM observation of vector/pDNA polyplexes. This material is available free of charge via the Internet at http://pubs.acs.org.

■ AUTHOR INFORMATION

Corresponding Authors

*E-mail: xshi@dhu.edu.cn.
*E-mail: lenat@uma.pt.

Notes

The authors declare no competing financial interest.

■ ACKNOWLEDGMENTS

This research was financially supported by the High-Tech Research and Development Program of China (2012AA030309), the National Natural Science Foundation of China (21273032), the Program for Professor of Special Appointment (Eastern Scholar) at Shanghai Institutions of Higher Learning, and the FCT-Fundação para a Ciência e a Tecnologia (through the projects PTDC/CTM-NAN/1748/2012 and PEst-OE/QUI/UI0674/2011-2013 (CQM pluriannual base funding)). X. Shi also thanks the Santander bank and the University of Madeira for the Invited Chair in Nanotechnology.

■ REFERENCES

(1) Caplan, A. I. Mesenchymal Stem Cells. *J. Orthop. Res.* **1991**, *9*, 641−650.
(2) Janderová, L.; McNeil, M.; Murrell, A. N.; Mynatt, R. L.; Smith, S. R. Human Mesenchymal Stem Cells as an in Vitro Model for Human Adipogenesis. *Obes. Res.* **2003**, *11*, 65−74.
(3) Pittenger, M. F.; Mackay, A. M.; Beck, S. C.; Jaiswal, R. K.; Douglas, R.; Mosca, J. D.; Moorman, M. A.; Simonetti, D. W.; Craig, S.; Marshak, D. R. Multilineage Potential of Adult Human Mesenchymal Stem Cells. *Science* **1999**, *284*, 143−147.
(4) Rickard, D. J.; Sullivan, T. A.; Shenker, B. J.; Leboy, P. S.; Kazhdan, I. Induction of Rapid Osteoblast Differentiation in Rat Bone Marrow Stromal Cell Cultures by Dexamethasone and BMP-2. *Dev. Biol.* **1994**, *161*, 218−228.
(5) Wang, S. G.; Castro, R.; An, X.; Song, C. L.; Luo, Y.; Shen, M. W.; Tomás, H.; Zhu, M. F.; Shi, X. Y. Electrospun Laponite-Doped Poly (lactic-co-glycolic acid) Nanofibers for Osteogenic Differentiation of Human Mesenchymal Stem Cells. *J. Mater. Chem.* **2012**, *22*, 23357−23367.
(6) Caplan, A. I. Adult Mesenchymal Stem Cells for Tissue Engineering Versus Regenerative Medicine. *J. Cell. Physiol.* **2007**, *213*, 341−347.
(7) Ponticiello, M. S.; Schinagl, R. M.; Kadiyala, S.; Barry, F. P. Gelatin-Based Resorbable Sponge as a Carrier Matrix for Human Mesenchymal Stem Cells in Cartilage Regeneration Therapy. *J. Biomed. Mater. Res.* **2000**, *52*, 246−255.
(8) Santos, J. L.; Oramas, E.; Pêgo, A. P.; Granja, P. L.; Tomás, H. Osteogenic Differentiation of Mesenchymal Stem Cells Using PAMAM Dendrimers as Gene Delivery Vectors. *J. Controlled Release* **2009**, *134*, 141−148.
(9) Santos, J. L.; Pandita, D.; Rodrigues, J.; Pêgo, A. P.; Granja, P. L.; Balian, G.; Tomás, H. Receptor-Mediated Gene Delivery using PAMAM Dendrimers Conjugated with Peptides Recognized by Mesenchymal Stem Cells. *Mol. Pharmaceutics* **2010**, *7*, 763−774.
(10) Shakhbazau, A.; Shcharbin, D.; Seviaryn, I.; Goncharova, N.; Kosmacheva, S.; Potapnev, M.; Gabara, B.; Ionov, M.; Bryszewska, M. Use of Polyamidoamine Dendrimers to Engineer BDNF-Producing Human Mesenchymal Stem Cells. *Mol. Biol. Rep.* **2010**, *37*, 2003−2008.
(11) Tomalia, D. A. Birth of a New Macromolecular Architecture: Dendrimers as Quantized Building Blocks for Nanoscale Synthetic Polymer Chemistry. *Prog. Polym. Sci.* **2005**, *30*, 294−324.
(12) Tomalia, D. A.; Frechet, J. M. J. *Dendrimers and Other Dendritic Polymers*; John Wiley & Sons Ltd: New York, 2001.
(13) Chen, Q.; Li, K.; Wen, S.; Liu, H.; Peng, C.; Cai, H.; Shen, M.; Zhang, G.; Shi, X. Targeted CT/MR Dual Mode Imaging of Tumors Using Multifunctional Dendrimer-Entrapped Gold Nanoparticles. *Biomaterials* **2013**, *34*, 5200−5209.
(14) Majoros, I. J.; Williams, C. R.; Baker, J. R.; James, R. Current Dendrimer Applications in Cancer Diagnosis and Therapy. *Curr. Top. Med. Chem.* **2008**, *8*, 1165−1179.
(15) Peng, C.; Qin, J.; Zhou, B.; Chen, Q.; Shen, M.; Zhu, M.; Lu, X.; Shi, X. Targeted Tumor CT Imaging Using Folic Acid-Modified PEGylated Dendrimer-Entrapped Gold Nanoparticles. *Polym. Chem.* **2013**, *4*, 4412−4424.
(16) Peng, C.; Zheng, L.; Chen, Q.; Shen, M.; Guo, R.; Wang, H.; Cao, X.; Zhang, G.; Shi, X. PEGylated Dendrimer-Entrapped Gold Nanoparticles for in Vivo Blood Pool and Tumor Imaging by Computed Tomography. *Biomaterials* **2012**, *33*, 1107−1119.
(17) Qiao, Z.; Shi, X. Dendrimer-Based Molecular Imaging Contrast Agents. *Prog. Polym. Sci.* **2014**, DOI: 10.1016/j.progpolymsci.2014.08.002.
(18) Shen, M.; Shi, X. Dendrimer-Based Organic/Inorganic Hybrid Nanoparticles in Biomedical Applications. *Nanoscale* **2010**, *2*, 1596−1610.
(19) Wolinsky, J. B.; Grinstaff, M. W. Therapeutic and Diagnostic Applications of Dendrimers for Cancer Treatment. *Adv. Drug Delivery Rev.* **2008**, *60*, 1037−1055.
(20) Beezer, A. E.; King, A. S. H.; Martin, I. K.; Mitchel, J. C.; Twyman, L. J.; Wain, C. F. Dendrimers as Potential Drug Carriers; Encapsulation of Acidic Hydrophobes within Water Soluble PAMAM Derivatives. *Tetrahedron* **2003**, *59*, 3873−3880.
(21) Twyman, L. J.; Beezer, A. E.; Esfand, R.; Hardy, M. J.; Mitchell, J. C. The Synthesis of Water Soluble Dendrimers, and Their Application as Possible Drug Delivery Systems. *Tetrahedron Lett.* **1999**, *40*, 1743−1746.
(22) Wang, Y.; Cao, X.; Guo, R.; Shen, M.; Zhang, M.; Zhu, M.; Shi, X. Targeted Delivery of Doxorubicin into Cancer Cells Using a Folic Acid−Dendrimer Conjugate. *Polym. Chem.* **2011**, *2*, 1754−1760.
(23) Wang, Y.; Guo, R.; Cao, X.; Shen, M.; Shi, X. Encapsulation of 2-Methoxyestradiol within Multifunctional Poly (amidoamine) Dendrimers for Targeted Cancer Therapy. *Biomaterials* **2011**, *32*, 3322−3329.
(24) Zheng, Y.; Fu, F.; Zhang, M.; Shen, M.; Zhu, M.; Shi, X. Multifunctional Dendrimers Modified with Alpha-Tocopheryl Succinate for Targeted Cancer Therapy. *Med. Chem. Commun.* **2014**, *5*, 879−885.
(25) Zhu, J.; Shi, X. Dendrimer-Based Nanodevices for Targeted Drug Delivery Applications. *J. Mater. Chem. B* **2013**, *1*, 4199−4211.
(26) Zhu, J. Y.; Zheng, L. F.; Wen, S. H.; Tang, Y. Q.; Shen, M. W.; Zhang, G. X.; Shi, X. Y. Targeted Cancer Theranostics Using Alpha-Tocopheryl Succinate-Conjugated Multifunctional Dendrimer-Entrapped Gold Nanoparticles. *Biomaterials* **2014**, *35*, 7635−7646.

DOI: 10.1021/am508760w
ACS Appl. Mater. Interfaces 2015, 7, 4833−4843

(27) Braun, C. S.; Vetro, J. A.; Tomalia, D. A.; Koe, G. S.; Koe, J. G.; C, R. M. Structure/Function Relationships of Polyamidoamine/DNA Dendrimers as Gene Delivery Vehicles. *J. Pharm. Sci.* **2005**, *94*, 423−436.
(28) Dufès, C.; Uchegbu, L. F.; Schätzlein, A. G. Dendrimers in Gene Delivery. *Adv. Drug Delivery Rev.* **2005**, *57*, 2177−2202.
(29) Huang, R. Q.; Qu, Y. H.; Ke, W. L.; Zhu, J. H.; Pei, Y. Y.; Jiang, C. Efficient Gene Delivery Targeted to the Brain Using a Transferrin-Conjugated Polyethyleneglycol-Modified Polyamidoamine Dendrimer. *FASEB J.* **2007**, *21*, 1117−1125.
(30) Lee, C. C.; MacKay, J. A.; Fréchet, J. M. J.; Szoka, F. C. Designing Dendrimers for Biological Applications. *Nat. Biotechnol.* **2005**, *23*, 1517−1526.
(31) Shan, Y. B.; Luo, T.; Peng, C.; Sheng, R. L.; Cao, A. M.; Cao, X. Y.; Shen, M. W.; Guo, R.; Tomás, H.; Shi, X. Y. Gene Delivery Using Dendrimer-Entrapped Gold Nanoparticles as Nonviral Vectors. *Biomaterials* **2012**, *33*, 3025−3035.
(32) Xiao, T. Y.; Hou, W. X.; Cao, X. Y.; Wen, S. H.; Shen, M. W.; Shi, X. Y. Dendrimer-Entrapped Gold Nanoparticles Modified with Folic Acid for Targeted Gene Delivery Applications. *Biomater. Sci.* **2013**, *1*, 1172−1180.
(33) Wang, W.; Xiong, W.; Wan, J. L.; Sun, X. H.; Xu, H. B.; Yang, X. L. The Decrease of PAMAM Dendrimer-Induced Cytotoxicity by PEGylation via Attenuation of Oxidative Stress. *Nanotechnology* **2009**, *20*, 105−103.
(34) Liu, H.; Wang, H.; Xu, Y.; Guo, R.; Wen, S.; Huang, Y.; Liu, W.; Shen, M.; Zhao, J.; Zhang, G.; Shi, X. Lactobionic Acid-Modified Dendrimer-Entrapped Gold Nanoparticles for Targeted Computed Tomography Imaging of Human Hepatocellular Carcinoma. *ACS Appl. Mater. Interfaces* **2014**, *6*, 6944−6953.
(35) Liu, H.; Wang, H.; Xu, Y.; Shen, M.; Zhao, J.; Zhang, G.; Shi, X. Synthesis of PEGylated Low Generation Dendrimer-Entrapped Gold Nanoparticles for CT Imaging Applications. *Nanoscale* **2014**, *6*, 4521−4526.
(36) Wen, S.; Li, K.; Cai, H.; Chen, Q.; Shen, M.; Huang, Y.; Peng, C.; Hou, W.; Zhu, M.; Zhang, G.; Shi, X. Multifunctional Dendrimer-Entrapped Gold Nanoparticles for Dual Mode CT/MR Imaging Applications. *Biomaterials* **2013**, *34*, 1570−1580.
(37) Cao, Y.; He, Y.; Liu, H.; Luo, Y.; Shen, M.; Xia, J.; Shi, X. Targeted CT Imaging of Human Hepatocellular Carcinoma Using Low-Generation Dendrimer-Entrapped Gold Nanoparticles Modified with Lactobionic Acid. *J. Mater. Chem. B* **2015**, *3*, 286−295.
(38) Qi, R.; Gao, Y.; Tang, Y.; He, R. R.; Liu, T. L.; He, Y.; Sun, S.; Li, B. Y.; Li, Y. B.; Liu, G. PEG-Conjugated PAMAM Dendrimers Mediate Efficient Intramuscular Gene Expression. *AAPS J.* **2009**, *11*, 395−405.
(39) Jeong, J. H.; Kim, S. W.; Park, T. G. Novel Intracellular Delivery System of Antisense Oligonucleotide by Self-Assembled Hybrid Micelles Composed of DNA/PEG Conjugate and Cationic Fusogenic Peptide. *Bioconjugate Chem.* **2003**, *14*, 473−479.
(40) Garg, A.; Tisdale, A. W.; Haidari, E.; Kokkoli, E. Targeting Colon Cancer Cells Using PEGylated Liposomes Modified with a Fibronectin-Mimetic Peptide. *Int. J. Pharm.* **2009**, *366*, 201−210.
(41) Otsuka, H.; Nagasaki, Y.; Kataoka, K. PEGylated Nanoparticles for Biological and Pharmaceutical Applications. *Adv. Drug Delivery Rev.* **2003**, *55*, 403−419.
(42) Tobio, M.; Gref, R.; Sanchez, A.; Langer, R.; Alonso, M. J. Stealth PLA-PEG Nanoparticles as Protein Carriers for Nasal Administration. *Pharm. Res.* **1998**, *15*, 270−275.
(43) Cai, W.; Chen, X. Anti-Angiogenic Cancer Therapy Based on Integrin Alphavbeta3 Antagonism. *Anticancer Agents Med. Chem.* **2006**, *6*, 407−428.
(44) Dechantsreiter, M. A.; Planker, E.; Mathä, B.; Lohof, E.; Hölzemann, G.; Jonczyk, A.; Goodman, S. L.; Kessler, H. N-Methylated Cyclic RGD Peptides as Highly Active and Selective $\alpha v\beta 3$ Integrin Antagonists. *J. Med. Chem.* **1999**, *42*, 3033−3040.
(45) Gronthos, S.; Simmons, P. J.; Graves, S. E.; G. Robey, P. Integrin-Mediated Interactions between Human Bone Marrow Stromal Precursor Cells and the Extracellular Matrix. *Bone* **2001**, *28*, 174−181.
(46) He, X.; Alves, C.; Oliveira, N.; Rodrigues, J.; Zhu, J.; Bányai, I.; Tomás, H.; Shi, X. RGD Peptide-Modified Multifunctional Dendrimer Platform for Drug Encapsulation and Targeted Inhibition of Cancer Cells. *Colloids Surf., B* **2015**, *125*, 82−89.
(47) Shukla, R.; Hill, E.; Shi, X.; Kim, J.; Muniz, M. C.; Sun, K.; Baker, J. R., Jr. Tumor Microvasculature Targeting with Dendrimer-Entrapped Gold Nanoparticles. *Soft Matter* **2008**, *4*, 2160−2163.
(48) Cao, X.; Shen, M.; Zhang, X.; Hu, J.; Wang, J.; Shi, X. Effect of the Surface Functional Groups of Dendrimer-Entrapped Gold Nanoparticles on the Improvement of PCR. *Electrophoresis* **2012**, *33*, 2598−2603.
(49) Chen, J.; Cao, X.; Guo, R.; Shen, M.; Peng, C.; Xiao, T.; Shi, X. A Highly Effective Polymerase Chain Reaction Enhancer Based on Dendrimer-Entrapped Gold Nanoparticles. *Analyst* **2012**, *137*, 223−228.
(50) Guo, S. T.; Huang, Y. Y.; Jiang, Q.; Sun, Y.; Deng, L. D.; Liang, Z. C.; Du, Q.; Xing, J. F.; Zhao, Y. L.; Wang, P. C. Enhanced Gene Delivery and SiRNA Silencing by Gold Nanoparticles Coated with Charge-Reversal Polyelectrolyte. *ACS Nano* **2010**, *4*, 5505−5511.
(51) Wen, S.; Zhao, Q.; An, X.; Zhu, J.; Hou, W.; Li, K.; Huang, Y.; Shen, M.; Zhu, W.; Shi, X. Multifunctional PEGylated Multiwalled Carbon Nanotubes for Enhanced Blood Pool and Tumor MR Imaging. *Adv. Healthcare Mater.* **2014**, *3*, 1568−1577.
(52) Shi, X.; Briseno, A. L.; Sanedrin, R. J.; Zhou, F. Formation of Uniform Polyaniline Thin Shells and Hollow Capsules Using Polyelectrolyte-Coated Microspheres as Templates. *Macromolecules* **2003**, *36*, 4093−4098.
(53) Hong, S. P.; Bielinska, A. U.; Mecke, A.; Keszler, B.; Beals, J. L.; Shi, X. Y.; Balogh, L.; Orr, B. G.; Baker, J. R.; Holl, M. M. B. Interaction of Poly(amidoamine) Dendrimers with Supported Lipid Bilayers and Cells: Hole Formation and the Relation to Transport. *Bioconjugate Chem.* **2004**, *15*, 774−782.
(54) Kim, T.-i.; Seo, H. J.; Choi, J. S.; Jang, H.-S.; Baek, J.-u.; Kim, K.; Park, J.-S. PAMAM-PEG-PAMAM: Novel Triblock Copolymer as a Biocompatible and Efficient Gene Delivery Carrier. *Biomacromolecules* **2004**, *5*, 2487−2492.
(55) Yan, G.; Arelly, N.; Farhan, N.; Lobo, S.; Li, H. Enhancing DNA Delivery into the Skin with a Motorized Microneedle Device. *Eur. J. Pharm. Sci.* **2014**, *52*, 215−222.
(56) Yi, W.-J.; Zhang, Q.-F.; Zhang, J.; Liu, Q.; Ren, L.; Chen, Q.-M.; Guo, L.; Yu, X.-Q. Cyclen-Based Lipidic Oligomers as Potential Gene Delivery Vehicles. *Acta Biomater.* **2014**, *10*, 1412−1422.
(57) Reseland, J. E.; Syversen, U.; Bakke, I.; Qvigstad, G.; Eide, L. G.; Hjertner, Ø.; Gordeladze, J. O.; Drevon, C. A. Leptin is Expressed in and Secreted from Primary Cultures of Human Osteoblasts and Promotes Bone Mineralization. *J. Bone Miner. Res.* **2001**, *16*, 1426−1433.
(58) Haba, Y.; Kojima, C.; Harada, A.; Ura, T.; Horinaka, H.; Kono, K. Preparation of Poly(ethylene glycol)-Modified Poly(amido amine) Dendrimers Encapsulating Gold Nanoparticles and Their Heat-Generating Ability. *Langmuir* **2007**, *23*, 5243−5246.
(59) Li, J.; Hu, Y.; Yang, J.; Wei, P.; Sun, W.; Shen, M.; Zhang, G.; Shi, X. Hyaluronic Acid-Modified Fe3O4@Au Core/Shell Nanostars for Multimodal Imaging and Photothermal Therapy of Tumors. *Biomaterials* **2015**, *38*, 10−21.

DOI: 10.1021/am508760w
ACS Appl. Mater. Interfaces 2015, 7, 4833−4843